Unclassified
SECURITY CLASSIFICATION OF THIS PAGE

REPORT DOCUMENTATION PAGE

AD-A205 326

1b. RESTRICTIVE MARKINGS

3. DISTRIBUTION / AVAILABILITY OF REPORT
Approved for public release;
Distribution unlimited

4. PERFORMING ORGANIZATION REPORT NUMBER(S)
AFGL-TR-89-0060

5. MONITORING ORGANIZATION REPORT NUMBER(S)

6a. NAME OF PERFORMING ORGANIZATION
Air Force Geophysics Laboratory

6b. OFFICE SYMBOL (If applicable)

7a. NAME OF MONITORING ORGANIZATION

6c. ADDRESS (City, State, and ZIP Code)
Hanscom AFB
Massachusetts 01731-5000

7b. ADDRESS (City, State, and ZIP Code)

8a. NAME OF FUNDING / SPONSORING ORGANIZATION

8b. OFFICE SYMBOL (If applicable)

9. PROCUREMENT INSTRUMENT IDENTIFICATION NUMBER

8c. ADDRESS (City, State, and ZIP Code)

10. SOURCE OF FUNDING NUMBERS

PROGRAM ELEMENT NO.	PROJECT NO.	TASK NO.	WORK UNIT ACCESSION NO.
61102F	2311	G3	24

11. TITLE (Include Security Classification) Image Processing of Coronal Pictures

12. PERSONAL AUTHOR(S) Olga Koutchmy*; Serge Koutchmy**; Christian Nitschelm§; Julius Sykora+; Raymond N.Smartt

13a. TYPE OF REPORT	13b. TIME COVERED	14. DATE OF REPORT (Year, Month, Day)	15. PAGE COUNT
REPRINT	FROM ____ TO ____	1989 February 28	11

16. SUPPLEMENTARY NOTATION * Lab Analyse Numerique Univ, Paris VI, France; **Paris Inst d'Astrophysique CNRS, France; § Institut d'Astrophysique, CNRS, France; +Astronomical Inst, Tatranska Lomnica, Czechoslovakia
Reprinted from Solar&Stellar Coronal Structure&Dynamics: A Festschrift in Honor of (OVER)

17 COSATI CODES			18. SUBJECT TERMS (Continue on reverse if necessary and identify by block number)
FIELD	GROUP	SUB-GROUP	Image processing, Solar corona

19. ABSTRACT (Continue on reverse if necessary and identify by block number)

Coronal images contain many complex, superposed, faint, optically-thin structures: rays, loops, curved streamers, etc. The spatial resolution is often limited by the signal/noise ratio in the recording medium while the dynamic range in intensity is severely dominated by the radial gradient. ~~We present~~ the results obtained with a new simple image processing algorithm applied to several typical eclipse and coronographic pictures. This 2D filter (second order difference operator in k-direction) shows superior quality by improving the signal/noise ratio, reducing the dynamic range and enhancing faint coronal structures. A comparison with results obtained with more commonly used 2D filters is also presented. ~~We describe briefly~~ the algorithm used here, together with discussions of enhanced coronal images of coronal physics interest.

20. DISTRIBUTION / AVAILABILITY OF ABSTRACT
☐ UNCLASSIFIED/UNLIMITED ☐ SAME AS RPT. ☐ DTIC USERS

21. ABSTRACT SECURITY CLASSIFICATION
Unclassified

22a. NAME OF RESPONSIBLE INDIVIDUAL	22b. TELEPHONE (Include Area Code)	22c. OFFICE SYMBOL
Richard C. Altrock		AFGL/PHS

DD FORM 1473, 84 MAR 83 APR edition may be used until exhausted. All other editions are obsolete.

SECURITY CLASSIFICATION OF THIS PAGE
Unclassified

89 3 07 033

CONT OF BLOCK 19:

Dr John W. Evans (R.C.Altrock, ed) National Solar Observatory, Sunspot, NM, pp 256-266, 1988

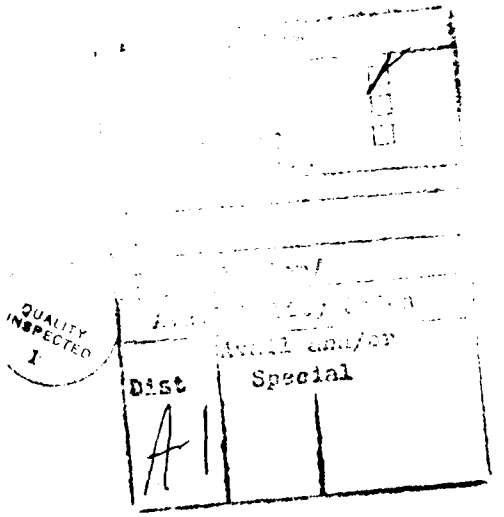

IMAGE PROCESSING OF CORONAL PICTURES

Olga Koutchmy

NSO/SP, Sunspot, NM 88349 and Lab. Analyse Numerique
Univ. Paris VI, France

Serge Koutchmy

NAS/NRC Resident Research Ass.
AFGL/NSO/SP, Sunspot, NM 88349 and Paris Inst. d'Astrophysique
CNRS - France

Christian Nitschelm

Summer Student at NSO/SP, Sunspot, NM 88349
Address: Institut d'Astrophysique, CNRS, France

Julius Sykora

Astronomical Institute,
Tatranska Lomnica, Czechoslovakia 05960

Raymond N. Smartt

National Solar Observatory[1], Sunspot, NM 88349

ABSTRACT: Coronal images contain many complex, superposed, faint, optically-thin structures: rays, loops, curved streamers, etc. The spatial resolution is often limited by the signal/noise ratio in the recording medium while the dynamic range in intensity is severly dominated by the radial gradient. We present the results obtained with a new simple image processing algorithm applied to several typical eclipse and coronographic pictures. This 2D filter (second order difference operator in k-direction) shows superior quality by improving the signal/noise ratio, reducing the dynamic range and enhancing faint coronal structures. A comparison with results obtained with more commonly used 2D filters is also presented. We describe briefly the algorithm used here, together with discussions of enhanced coronal images of coronal physics interest.

[1]Operated by the Association of Universities for Research in Astronomy, Inc. under contract with the National Science Foundation

1. Introduction

The extraction of precise parameters (intensity distribution over a cross-section, shape, size, direction, etc.) from coronal images, both for white-light and emission-line studies, is difficult unless some image processing technique is applied. For example,the structures to be studied are optically thin and superposed structures can reproduce rather large modulations. Additionally, the steep radial gradient of intensities can mask details of the inner coronal structure, while other details can be lost. Further, because the radiations are faint and because the most popular detector in coronal imaging is photographic film with its rather low quantum efficiency, (the use of CCD cameras, with all their special characteristics, is not considered here), pictures are often noisy, with variable signal-to-noise ratio. Here we present the results of some attempts, including the use of an apparently novel algorithm, to improve coronal pictures in order to try to answer several outstanding questions concerned with different aspects of the coronal physics.

Even in the case of images recorded in the brightest visible line, 530.3nm of Fe XIV, some image processing can be valuable; the interpretation of detailed structure, such as interacting post-flare loops, is otherwise extremely difficult, and it is virtually essential in comparative line studies, especially in investigations of temperature and density inhomogeneities. Figure 1 shows a part of a picture taken by one of us (J.S.) during the solar total eclipse of July 31, 1981, with a 3Å bandwidth 530.3 nm filter. The picture was processed using different methods, including the commonly used method of high pass filtering (see figure 2). Based on the results of applying such different methods of processing, largely described in books like the classical monograph of Rosenfeld and Kak, 1976, or those of Coster and Chermant, 1985, we have investigated a more empirical approach, taking into account the anisotropic properties (due to the dominance of magnetic field effects and the dynamical characteristics of the corona) of the structures in the solar corona.

An example of the result obtained with this apparently novel algorithm, which we call "MaD MAXII" (multi-directional maximum of second derivatives) is shown on figure 1, part d, as compared with the results of applications of more commonly used algorithms. Since we believe our algorithm is superior, we present a brief description of the method before commenting on its application in several interesting cases, as well as some unsuccessful attempts.

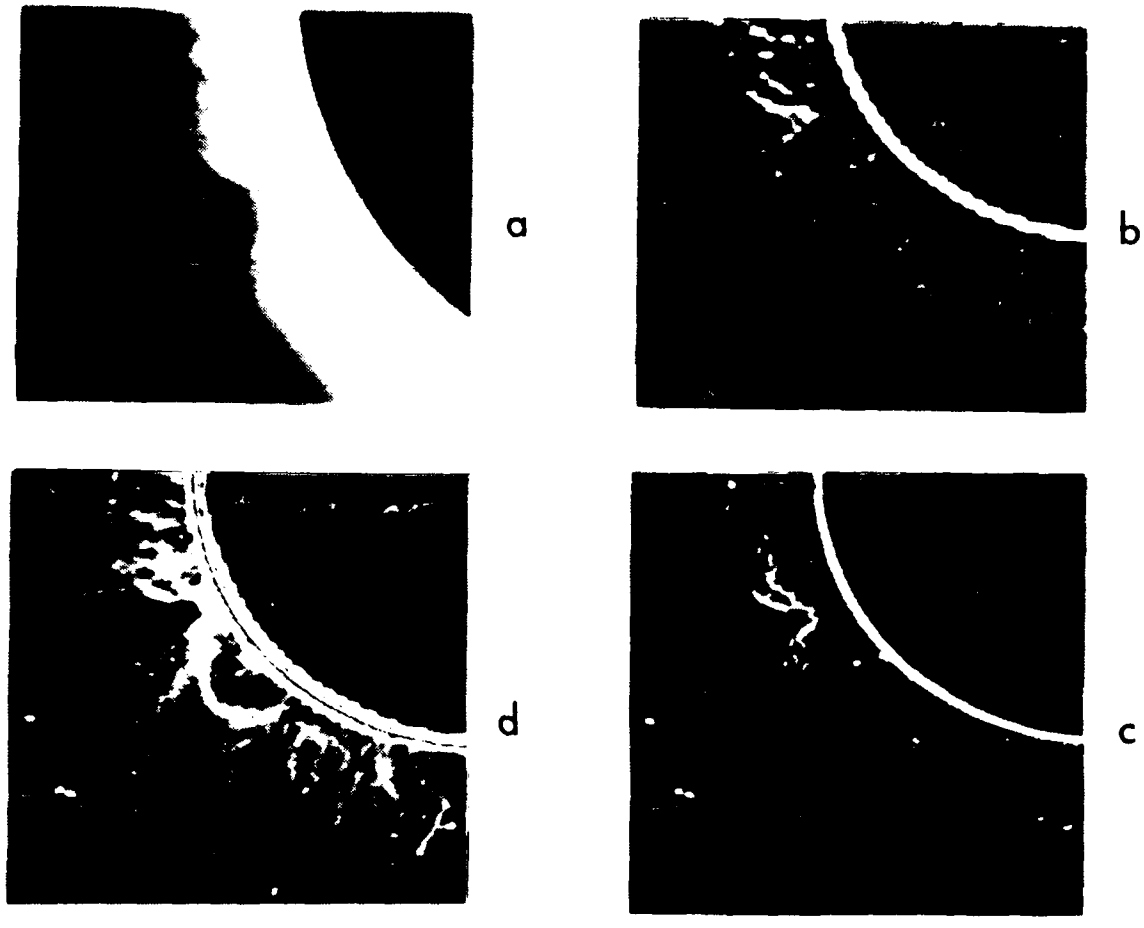

Figure 1. Example of image processing of a typical coronal picture using different algorithms:

a. Original picture taken during the July 31st,1981 Solar eclipse (J. Sykora) in the light of Fe XIV emissions at 530.3 nm;
b. Image obtained with a laplacian filter;
c. Image obtained using the "multidirectional maximum of absolute derivatives" (J.M. Malherbe and al.,1986);
d. Image obtained using the proposed algorithm ("madmax").
Note that high pass or pass band filters give more noisy results: see Fig.2

2- Brief description of the proposed image processing

The purpose of the processing is to find ,as far as possible, the detailed distribution of different features (curved or straight,aligned or not) of variable sizes which typically intersect. These features are distributed over a noisy picture with a variable in intensity background.For such an application,the use of the second derivatives technique seems appropriate. For digital pictures differences must be used rather than derivatives. The features can be oriented in any direction;to find this orientation we compute the second order differences in 8 directions and choose those for which the values are maximum.

We shall now show in more detail how the processing works.

Let g(x,y) be the matrix of measured intensities. The algorithm uses the following operator M defined by:

$$M(g)=\alpha M8(g)+\beta E2(M8(S2(g)))+\gamma E4(M8(S2(S2(g))))+...$$

where:

-> $M8 = \max(- \Delta_k^2)$

with Δ_k^2 the second order difference operator

in the k -direction defined by the angle $k\,\Pi/8$, $k=0,1,...,7$.

-> S2 is the operator which averages every 2 rows and every 2 columns of a matrix to make a single row and a single column.

-> E2 and E4 are the operators which expand a matrix by bilinear interpolation with the row and column expansion factor equal to 2 and 4 respectively.

-> α , β , γ are some weights taking the values 0,1,2,... depending on the signal to noise ratio and on the relative dimensions of the picture features.

The operator M is non linear, it is based upon the anisotropic operator max and it is shift-invariant and non idempotant.

The effect of M on a picture can be understood by considering a simple one-dimensional example. Then M8 is computed only in one direction and its effect will be to amplify "convex" and "concave" points. Thus its purpose is the detection of places where there is a significant change in gray level. So the meaning of the processing in terms of image sharpening is quite obvious.

Unfortunately,the algorithm uses a second order difference operator relatively sensitive to image noise, although the averaging operator S2 reduces this effect.

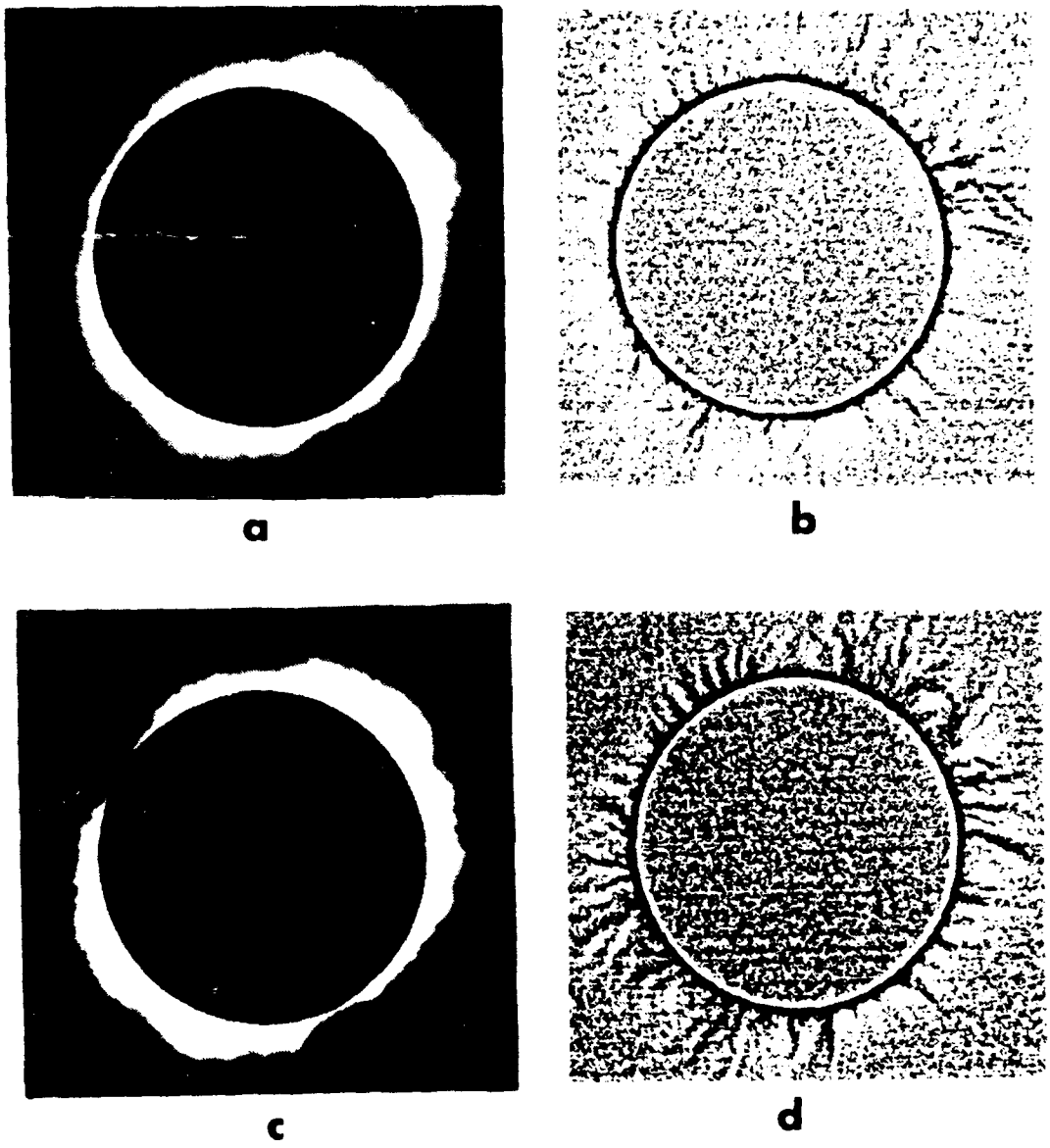

Figure 2. Image processing with a commonly used 2D filter (high pass) of 2 simultaneous eclipse monochromatic pictures obtained on July 31st,1981 (J. Sykora):

a. Original image in 637.4 nm of Fe X
(FWHM of the filter 0.3 nm);
North is at top left, East is at bottom left;
b. Processed image of a.;
c. Original image in 530.3 nm of Fe XIV
(FWHM of the filter 0.2 nm);
d. Processed image of c.;
Note the absence of correlations between the emissions of Fe X ($T \simeq 10^6$K) and the emissions of Fe XIV ($T \simeq 1.8 \times 10^6$K).

3. Discussion of results

a. Figure 2 shows full images obtained simultaneously in the green line (530.3nm) Fe XIV emitting preferentially at temperatures near 2.0 x 10^6 K (part c) and in the red line (637.4nm) of Fe X emitting near 1.2 x 10^6 K. Processed images (part b and d) with a "classical" high-pass filter in the Fourier space removes the radial gradient and shows convincingly the large spatial differentiation of locations emitting these two lines.

This makes rather doubtful results based on the use of the so-called line-ratio method to deduce the coronal temperature and abundances: structures emitting in one temperature "regime" do not spatially coincide with structures emitting in another, when ionization temperatures differ by a factor of 1.5 or more, as is the case for Fe X and Fe XIV.

Using the MaD MAX II program, we succeeded in showing the correlations between 530.3nm emission of Fe XIV and structures revealed by a corresponding white light picture (essentially electron density Ne, structures,). Figure 3 shows a part of the 530.3nm picture processed with MaD MAX II, as was the W.L. picture. Although the intensity modulations of the original pictures are very different (530.3nm emissions are a nearly quadratic function of the Ne distribution, while W.L. intensities are only a linear function of Ne). In addition, the two pictures were obtained using completely different methods and instruments. The structures revealed by the processing look very similar, confirming the excellence of the Fe XIV line as an indicator of the coronal density distribution and therefore, as a "good" line to be used for monitoring coronal holes (see R. Altrock, this volume). We do not know the exact origin of this correlation, but suspect that the most evident interpretation calls for a temperature "regime" of the solar corona that is optimum for Fe XIV emission, although this interpretatin should be tested using several other coronal lines such as those of Fe XIII in the UV or IR.

b. The use of the proposed algorithm appears to be very effective in the case of W.L. pictures, showing subtle details connected with dynamical processes such as coronal mass ejections, etc. Figures 4 and 5 show the images processed with MaD MAX II of a coronal mass ejection phenomena observed during the Feb. 16, 1980 total solar eclipse (the so-called "tennis-racket"event); this CME is studied elsewhere in this volume (see Koutchmy and Nitschelm), so we do not comment here on the scientific aspects of the result of the image processing. Observe, however, that the unprocessed picture does not reveal the event convincingly (compare with figure 5). However, the processed images (Figures 4 and 5) suggest an interpretation based on the twisting or reconnection processes and facilitate measurements of proper motions.

c. The last example, Figure 6, is an example of very interesting photographic images of Fe XIV, FeX and Hα emissions obtained with the "one-shot" coronagraph of Sacramento Peak (NSO) Observatory (see

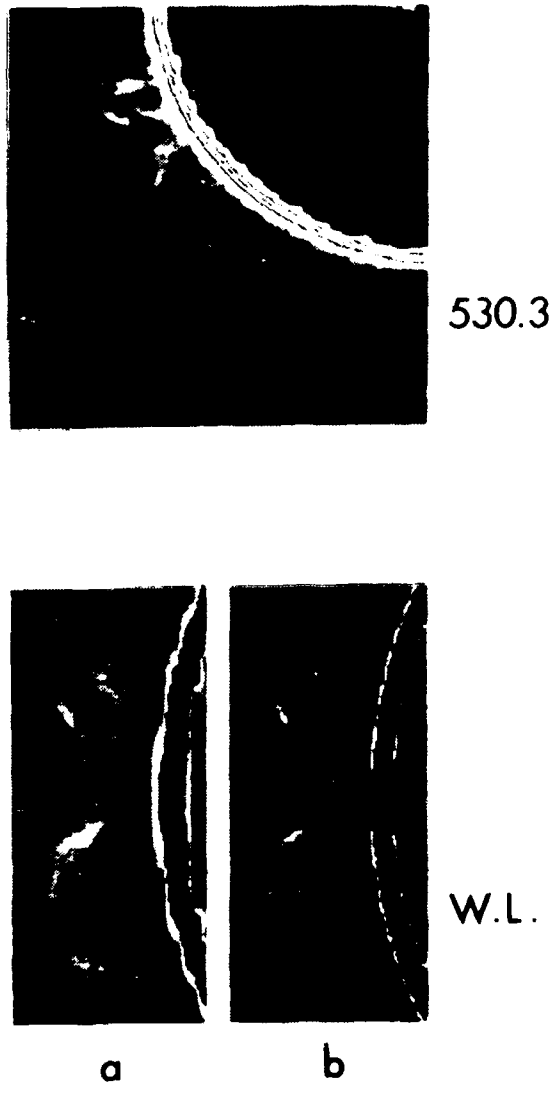

Figure 3. Comparison of different coronal emissions of the inner corona:

Upper part: processed image of 530.3 emissions of Fe XIV;
Lower part: processed image of white light intensities (density structures) using different weights (a&b).
Note the excellent correlations between the Fe XIV emissions and the density structures as shown on the white light picture.

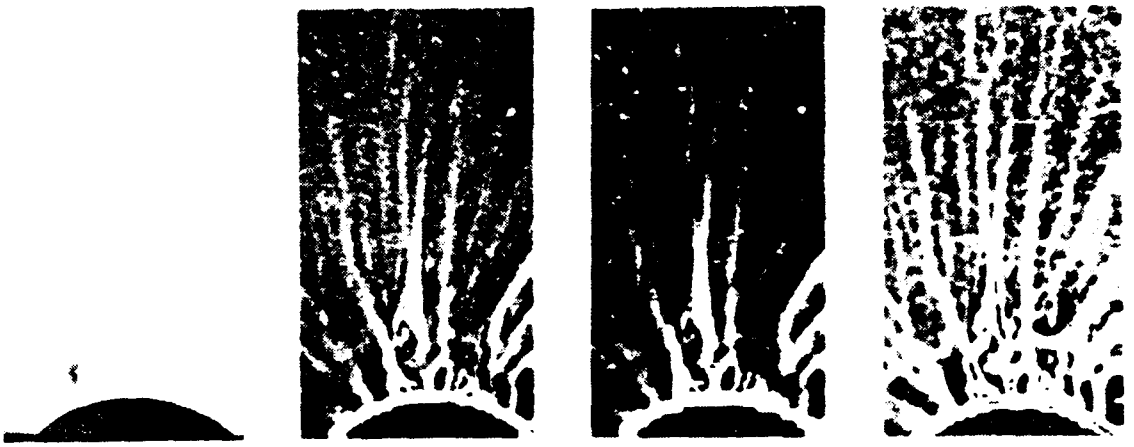

Figure 4. Morphological analysis of the legs of a coronal mass ejection event observed during the total solar eclipse of Feb.16.1980 (see Fig.4):

a. Part of an original picture taken by J. Dürst at 10h10 U.T.;
b..c..d. Processed images with different weights in the proposed algorithm ("madmax").
Note the twistings apparent in the processed images at the location of the legs of the C.M.E. shown on the Fig.5.

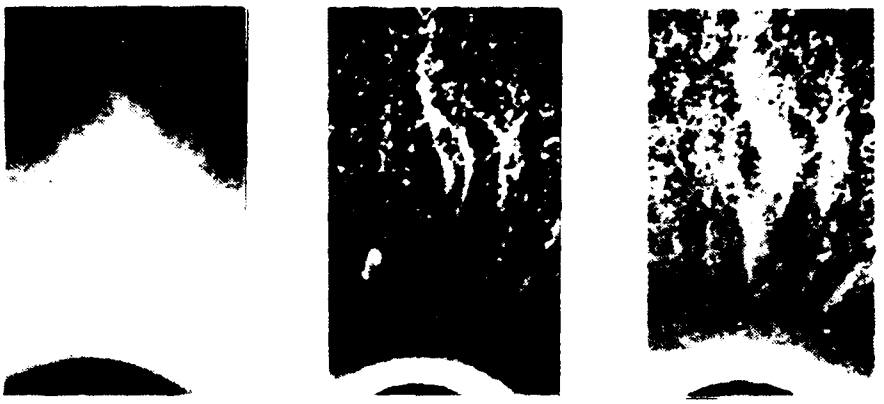

Figure 5. Morphological analysis of C.M.E. observed during the total solar eclipse of Feb.16, 1980:

a. Part of an original picture taken by F. Diego at 8h23 U.T.
b.,c. Processed images with different weights in the proposed algorithm ("madmax").

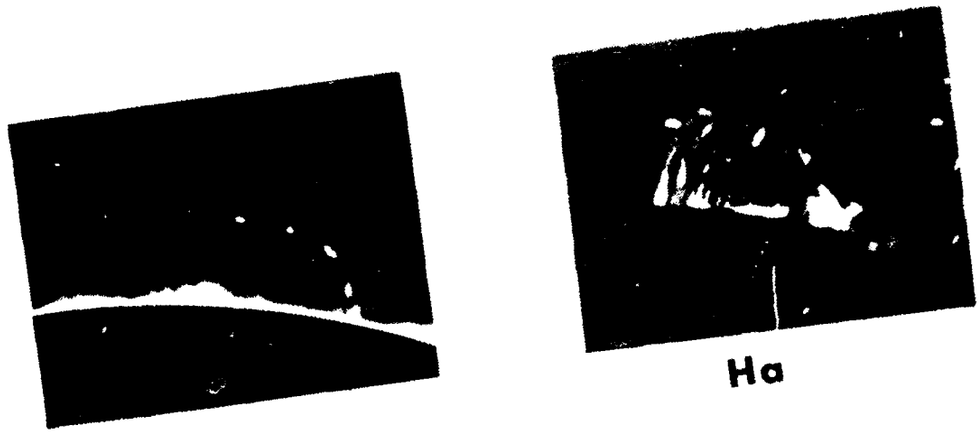

Figure 6. Attempt to relate the structure of Hα loops observed above an active region and coronal loops observed in the light of Fe XIV emission at 530.3nm. "One-shot" coronograph (SPO) observations (R. Smartt, 1980).
Note on the enlarged drawing that Hα loops are "contained" definitely inside the coronal loop system.

Smartt and Zhang, 1986), which have not yet been successfully processed. These pictures are recorded on 2415 film of very fine grain with a scale of 55 arcsec/mm. For several reasons, it has not been possible to digitize these images successfully with the fast microphotometer of SPO. Primarily, the small scale of the images is not fully resolved. An additional difficulty comes from the so-called "fringing effect" produced by the laser light used to scan the picture. Further, the overall density of the film is low (d< 0.2) and the range of photographic densities to be measured are small. We applied MaDMAXII to several digitized pictures and even more "classical" algorithms without great success. Disappointing results were obtained even when a magnified duplicate was used for the digitization. Figure 6 shows selected, highly magnified prints of images of great interest (other very interesting examples have also been studied, but they represent only a very small fraction of the data set available from this instrument. The sketch illustrates the kind of events that can only be studied accurately with processed images. It shows Hα emission of the cool part of the corona (indeed - loop-like prominence structures) contained within the system of coronal loops as evidence by their emissions in Fe XIV line. Such observations strongly suggest a "2-step" configuration of the magnetic field lines above an active region, substantially supporting the phenomenology and mechanism of CMEs recently suggested to explain the observation of prominence material behind transients. However, this somewhat rather speculative claim needs to be checked by comparing the morphological characteristics of the structure as revealed in the processed images. But for this we need an improved method for obtaining accurate digitized data.

4. References

M. Coster et J.-L. Chermant, "Precis d'analyse d'images", Editions du CNRS, 1985

J.M. Malherbe, J.C. Noens and Th. Roudier, "Numerical Image Processing Applied to the Solar Corona", Solar Physics, 102 (1986), 393-398

Rosenfeld A. and Kak A.C., "Digital picture processing", Academic Press, 1976

Smartt, R.N. and Zhenda Zhang, "Visible Coronal Emission Associated with a Quiescent Prominence", Solar Physics, 90, (1984), 315-324